ELSEVIER

Journal of Chromatography A, 875 (2000) 389–401

JOURNAL OF CHROMATOGRAPHY A

www.elsevier.com/locate/chroma

Chiral capillary electrophoretic analysis of the enantiomeric purity of a pharmaceutical compound using sulfated β-cyclodextrin

Lili Zhou*, Bruce D. Johnson[1], Carrie Miller, Jean M. Wyvratt

Merck Research Laboratories, Merck and Co. Inc., P.O. Box 2000, Rahway, NJ 07065, USA

Abstract

A practical chiral capillary electrophoresis method using randomly sulfated β-cyclodextrin was developed for the quantitative determination of the chiral purity of a pharmaceutical compound. A systematic method development approach was conducted by modifying selected parameters such as the concentration of the chiral selectors, buffer pH, organic modifiers, buffer concentrations and type, temperature and applied voltage. The results of the investigation permitted an improved understanding of the separation mechanism. Two facile strategies for the reversal of the enantiomer elution order are also described. The optimized method was validated in terms of variability of the chiral selector, linearity, sensitivity, accuracy, recovery, ruggedness, and precision.

Keywords: Pharmaceutical analysis; Enantiomer separation; Validation; Cyclodextrins; Aminoindanol; Spiro[2H-benzofuro(2,3-*a*)quinolizine-2,4′(1′H)pyrimidin]-2′(3′H)-one, 1,3,4,5′,6,6′,7,12*b*-octahydro-1′,3′dimethyl-, (2*S*-*trans*)-

1. Introduction

The chiral analysis of pharmaceutical compounds is a very important field of application, especially in the pharmaceutical industry, as frequently the two enantiomers possess different pharmacological properties. In the past several years, capillary electrophoresis (CE) has been established as a tool for enantiomeric analysis in addition to enantioselective GC and HPLC. The applications of CE have been extensively covered in recent reviews [1–4].

Cyclodextrins (CDs) are the most widely used chiral selectors in CE. Several applications of CE enantiomeric separations using neutral CDs have been successfully achieved in our laboratory in the past 2 years [5,6]. Recently, commercially available charged CDs have provided additional alternatives towards the development of fast, simple and efficient CE enantiomeric separation methods. The first application utilizing charged CDs was reported by Terabe [7]. Later on, Nardi et al. studied a positively charged β-CD on the resolution of several hydroxy acid enantiomers [8]. In the past several years, successful CE enantiomeric separations have been achieved by several laboratories using negatively charged sulfated β-CDs (S-β-CD) as described in recent reviews [1–4].

The development of practical CE methods using CDs for enantiomeric separation is facilitated if applicable theoretical models are available. Wren and Rowe described such a separation model for CE based on the formation of a 1:1 chiral selector–enantiomer (host–guest) complex [9]. Penn et al. refined this model and demonstrated how to determine binding constants from CE mobility data [10]. Rawjee et al. extended the model to include

*Corresponding author.

[1]Present address: Parke-Davis, Analytical Research and Development, 170 Tabor Road, Morris Plains, NJ 07950, USA.

0021-9673/00/$ – see front matter
PII: S0021-9673(99)01175-9

explicitly the effects of pH and concentration of chiral selector, and distinguished among cases in which the enantiomer complexation with the neutral CD occurs only with the undissociated forms of weak acid or weak base enantiomers, only with the dissociated form, or with both forms [11–13]. Recently, Vigh and coworkers developed a similar model for CE enantiomeric separations using charged CDs and a series of papers using this model (e.g. the CHARM ''charged resolving agent migration'' model) has been published [14–18]. Gahm and Stalcup [19,20] and Wang and Khaledi [21] also using Wren and Rowe's model described the CE enantiomeric separation behavior using randomly substituted charged CDs.

In this paper, we demonstrate a systematic approach to method development for the CE enantiomeric analysis of a pharmaceutical compound, compound I (Fig. 1a), using S-β-CD. The method is desired to separate the enantiomers and determine the purity of the desired enantiomer in order to ensure the quality of the synthetic product.

During our study, both single-isomer S-β-CD [15–17] and randomly substituted S-β-CDs were utilized. Various operating parameters, including both compositional [such as pH of the background electrolyte (BGE), concentration of chiral selectors, concentration of BGE and organic modifiers] and operational (such as temperature, electric field polarity, applied voltage and type of capillary) parameters, were selectively modified in order to gain a better understanding of the separation mechanisms. We found that the enantiomeric separation behaviors of compound I using randomly substituted charged CDs have very similar trends to the predictions of the CHARM model. Using another enantiomeric pair of pharmaceutically related compounds, *cis*-aminoindanol (Fig. 1b), a clear demonstration is provided of how a pair of cationic enantiomers transition from positively charged ions to negatively charged ions. Additionally, two different techniques to reverse the elution orders are provided. The optimized method was validated in terms of variability of the chiral selector, linearity, sensitivity, accuracy, recovery, ruggedness and precision.

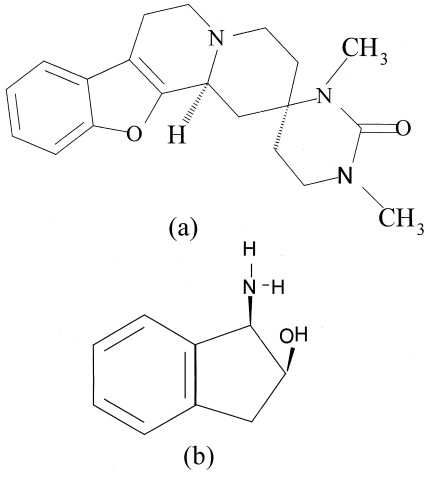

Fig. 1. Chemical structure of compound I (a) and (+)-*cis*-aminoindanol (b).

2. Experimental

2.1. Instrumentation

A Hewlett Packard ^{3D}CE (HP^{3D}, HPCE, Model G1600A; Hewlett Packard, Wilmington, DE, USA) system was used. Both fused-silica capillaries [56 cm effective length, 63 cm total length and 75 μm internal diameter (I.D.)] and polyvinyl alcohol (PVA) coated capillaries (56 cm effective length, 63 cm total length and 50 μm I.D.) were purchased from Hewlett-Packard. Data collection and analysis was performed with a PE Nelson data system equipped with AccessChrom software (version 1.9) (PE Nelson, Cupertino, CA, USA).

2.2. Reagents

Both compound I {spiro[2H-benzofuro(2,3-*a*)quinolizine-2,4′(1′H)pyrimidin]-2′(3′H)-one, 1,3,-4,5′,6,6′,7,12*b*-octahydro-1′,3′-dimethyl-, (2*S*-*trans*)-} and its enantiomer (pK_a=6.0) and (+)-*cis*-aminoindanol [*cis*-1(*R*)-amino-2(*S*)-indanol] and its enantiomer (pK_a=8.5) were prepared by the Process Research Department of Merck Research Laboratories (Rahway, NJ, USA). Heptakis(2,3-diacetyl-6-sulfato)-β-cyclodextrin (HDAS-β-CD), heptakis(2,3-dimethyl-6-sulfato)-β-cyclodextrin and heptakis-6-sulfato-β-cyclodextrin were purchased from Regis (Morton Grove, IL, USA) (for structures see Refs.

[15–17]). Two types of randomly S-β-CDs were purchased from Aldrich (Milwaukee, WI, USA) and Cerestar USA, (Hammond, IN, USA). Native neutral β-CD was purchased from Sigma (St. Louis, MO, USA). Phosphate buffers (50 m*M*, pH 2.5 and 7.0), Tris buffer (50 m*M*, pH 8.3), Tris–borate buffer (pH 9.3), 1 *M* and 0.1 *M* sodium hydroxide (NaOH) were purchased from Hewlett-Packard. Methanol (MeOH), ethanol (EtOH), isopropanol (IPA), acetonitrile (ACN), and triethylamine (TEA) were obtained from Fisher (Springfield, NJ, USA). Deionized (D.I.) water was obtained from a Milli-Q system (Millipore, Bedford, MA, USA).

2.3. Solutions

The diluent for all solution preparations was water–acetonitrile (90:10). An enantiomeric mixture standard solution was made by mixing authentic sample solutions of compound I and its enantiomer. Six linearity standard solutions containing compound I were prepared over the range from 0.1% to 125% of the target concentration of 0.5 mg/ml. The recovery test solutions contained 0.5 mg/ml compound I spiked with 0.1, 0.5 and 1.0% (w/w) of the minor enantiomer. The neutral marker of electroosmotic flow (EOF) was MeOH [24]. All solutions were filtered through a 0.45 μm nylon-66 membrane syringeless filter (Whatman, Clifton, NJ, USA).

2.4. Capillary preparation

New bare fused-silica capillaries were flushed with 1 *M* NaOH for 60 min followed by D.I. water for 10 min and 0.1 *M* NaOH for 30 min. New PVA capillaries were flushed with D.I. water for 30 min.

2.5. Electrophoretic separation conditions

Except when systematically varying the composition, the BGE used was 25 m*M* low-pH sodium phosphate buffer (pH 2.5) with 1.5% (w/w) S-β-CD. A diode array UV detector was set at wavelength 200 nm. Hydrodynamic sample injection was used with a 3-s injection time at 50 mbar pressure. The applied voltage was −15 kV (''reversed'' polarity, inject at cathode) unless otherwise specified. The capillary temperature was controlled at 30±0.1°C. The capillary was flushed/conditioned with the BGE for 10 min between injections.

3. Results and discussion

3.1. Selection of suitable CDs

Since the single-isomer sulfated cyclodextrins are reported to provide a more rugged separation selectivity from batch to batch [14–18], an initial separation attempt was made in CE using HDAS-β-CD based on the CHARM model. Three different pH (2.5, 7.0 and 8.3) BGEs were used. The concentration of HDAS-β-CD was varied between 5, 10, 20, 30 and 50 m*M*. Both polarities were tried with both neutral coated (PVA coated) and uncoated (fused-silica) capillaries. Unfortunately, no satisfactory separation between compound I and its enantiomer was readily achieved. The separation suffered from either poor efficiency or selectivity. Then the utilization of two types of randomly S-β-CDs was attempted. The first one from Cerestar was reported to have a degree of sulfation of about four and the second one from Aldrich was reported to have a degree of sulfation from seven to ten. Utilizing both brands of the randomly S-β-CDs, baseline separation between the enantiomers was readily achieved after preliminary method development. However, the enantiomeric resolution obtained from a CE system that used Aldrich's S-β-CD was found to be superior in comparison to Cerestar's product. Additionally, peak splitting was observed when low concentrations of the Cerestar's S-β-CD BGE were used. In order to clarify these differences, CE with indirect UV detection, as previously published [17] was used to determine the distributions of the degree of sulfation and overall purity of these S-β-CDs. HDAS-β-CD purchased from Regis was used as a control sample. The results revealed that both the Aldrich S-β-CD and HDAS-β-CD gave a major single peak with a purity greater than 95 area%. However, the Cerestar S-β-CD contained multiple peaks, which indicated it contained multiple degrees of sulfation. Based on the preliminary separation results and CD quality, the randomly S-β-CDs obtained from Aldrich were selected for both separation optimization and mechanism investigation.

3.2. Effect of S-β-CD concentration on the separation

The effect of the concentration of S-β-CD on the separation was explored on a bare silica capillary with the BGE pH 2.5 and the concentration of S-β-CD was varied from 0 to 4.0% (w/w). The change in effective mobilities for compound I and its enantiomer with increasing concentration of S-β-CD was plotted as shown in Fig. 2.

Since the S-β-CD was not a single isomer, the binding constants between the chiral resolving agent and the enantiomers could not be determined, thus limiting the direct application of the CHARM model. However, the separation trends that we observed were in good agreement with the theoretical predictions of the CHARM model.

Based on the CHARM model, for a cationic enantiomer pair with a single-isomer chiral selector, the separation selectivity is defined as $\alpha = \mu_D^{eff} / \mu_U^{eff}$ (where μ_D^{eff} and μ_U^{eff} are the effective mobilities of the desired/major and undesired/minor enantiomers, respectively). When the anionic single-isomer chiral resolving agent is added to the BGE and the concentration is increased, the effective mobilities of both enantiomers start to decrease from one to zero and then transition into an increase in the negative direction as the complexation occurs between the enantiomers and chiral selector. Simultaneously, α goes from one in the absence of the chiral selector through zero where the effective mobility of the later eluted (stronger-complexing) enantiomer becomes zero while the effective mobility of early eluted (weaker-complexing) enantiomer peak is still cationic. Then α becomes increasingly negative because the direction of the electrophoretic migration of the two enantiomers is in the opposite direction, with one of the enantiomers never reaching the detector without the presence of significant EOF. When the effective mobility of the weaker-binding enantiomer becomes zero, α approaches discontinuity and becomes an infinitely negative value. Upon further increasing the concentration of the S-β-CD and reversing the applied polarity, α becomes positive

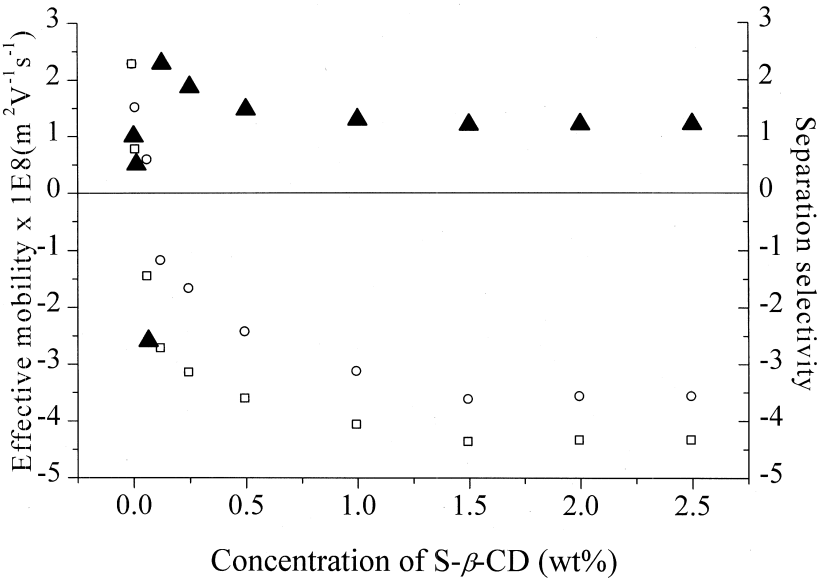

Fig. 2. Effect of the concentration of S-β-CD on enantiomer effective mobilities and separation selectivity, α, for compound I and its minor enantiomer. Open circle, effective mobility of the minor isomer; open square, effective mobility of the major isomer; solid up-triangle, α. Conditions: capillary, bare fused-silica 64.5 cm (effective length 56 cm)×75 μm I.D. at 30°C; BGE, 25 m*M* sodium phosphate buffer, pH 2.5; UV detection at 200 nm; injection, 50 mbar pressure for 3 s. The concentration of the S-β-CD was varied. Applied voltage: +15 kV from 0 to 0.065% (w/w) S-β-CD, −15 kV from 0.065 to 4.0% (w/w) S-β-CD.

and begins to level off towards the theoretical limit of $\alpha>1$, where both enantiomers are anionic and migrate in the same direction again [14].

The effective mobility and separation selectivity (α) curves provided in Fig. 2 demonstrate good agreement with the theoretical predictions. No difference in the effective mobilities of the two enantiomers, μ_D^{eff} and μ_U^{eff} was noted without the chiral selector present in the BGE ($\alpha=\mu_D^{eff}/\mu_U^{eff}=1$). Additionally, before the addition of S-β-CD into the BGE (pH 2.5), μ_D^{eff} and μ_U^{eff} were positive, verifying that both enantiomers were cationic ($pK_a=6.0$). As the concentration of the S-β-CD was increased, μ_D^{eff} and μ_U^{eff} began to decrease. At the concentration of S-β-CD=0.065% (w/w), only the weaker-binding enantiomer eluted under ''normal'' polarity (injected at anode), the stronger-binding enantiomer peak was detected only when ''reversed'' polarity (inject at cathode) was applied. The α was negative, indicating that compound I and its enantiomer migrated in opposite directions. At the concentration of S-β-CD=0.125% (w/w), both enantiomers migrated in the same direction (utilizing ''reversed'' polarity) and α became a positive number (2.2). As the concentration of S-β-CD increased further, α began to decrease and plateau to its limiting value (~1.2). The peak resolution reached a maximum when the enantiomers were close to the cationic-to-anionic cross-over point. However, the run time was excessive resulting in inefficient peak shape. Therefore, the concentration of S-β-CD of 1.5% (w/w) was selected for the final method that provided a compromise between sufficient resolution and run time. Importantly, this selection is in the middle of a plateau region of the μ^{eff}~[CD] plot. The S-β-CD concentrations of ±0.5% (w/w) provided almost equivalent separations, therefore, possible method variation caused by batch to batch S-β-CD variation as well as other factors were minimized.

In order to provide a concrete example of the transition of a pair of cationic enantiomers from positively charged ions to negatively charged ions, another enantiomeric pair of pharmaceutically related compounds, *cis*-aminoindanol, was investigated under a high pH BGE (pH_{app} 6.5). The pK_a of the *cis*-aminoindanol enantiomers is 8.5 and thus, they are fully protonated under the high pH BGE conditions. Fig. 3a clearly demonstrates the transition of the *cis*-aminoindanol enantiomers from cationic, to opposite polarities, to both becoming anionic. As the concentration of the S-β-CD increases, the initially positive charged enantiomers become negatively charged as described previously but they still reach the detector with ''normal'' polarity due to the high EOF present.

Fig. 3b demonstrates the change in effective mobilities and α for the *cis*-aminoindanol enantiomers with increasing concentration of the S-β-CD. The behavior of these curves is very similar to Fig. 2. The cationic effective mobilities of the *cis*-aminoindanol enantiomers decrease as the concentration of the S-β-CD is increased, then they transition to anionic mobility. In parallel, α decreases initially, then becomes negative at the cationic-to-anionic cross-over point on the mobility curve. As soon as both enantiomers are anionic, α becomes positive again. However, although α displayed discontinuity at the point where the effective mobility of the weaker complexed enantiomer equals zero, α did not approach an infinitely negative value due to the presence of significant EOF at pH 6.5 BGE. In fact, at the cationic-to-anionic cross-over point, both cationic and anionic peaks eluted out in same direction.

3.3. Effect of the BGE pH on the separation

Based on the CHARM model, by measuring the effective mobility over a wide pH range, one can learn whether only the unionized (type I), only the ionized (II), or both forms (III) associate selectively with the chiral selector [14]. The enantiomeric separation of compound I and its enantiomer were obtained in both the ionized (BGE pH 2.5) and unionized form (BGE pH 9.3) as given in Fig. 4a. Thus, the separation behavior is characteristic of the type III case.

Since both enantiomers become anionic upon complexation with S-β-CD at 1.5% (w/w), an additional study was carried out using a PVA coated capillary in which the EOF is nearly negligible ($0.4\cdot10^{-9}$ $m^2/V/s$ at pH_{app} 7.0). ''Reversed'' polarity was utilized and the pH_{app} was varied from 2.5 to 7.0 by mixing 25 m*M* low-pH (2.5) and 25 m*M* high-pH (7.0) phosphate buffers. As displayed in Fig. 4b, the absolute effective mobilities decreased as

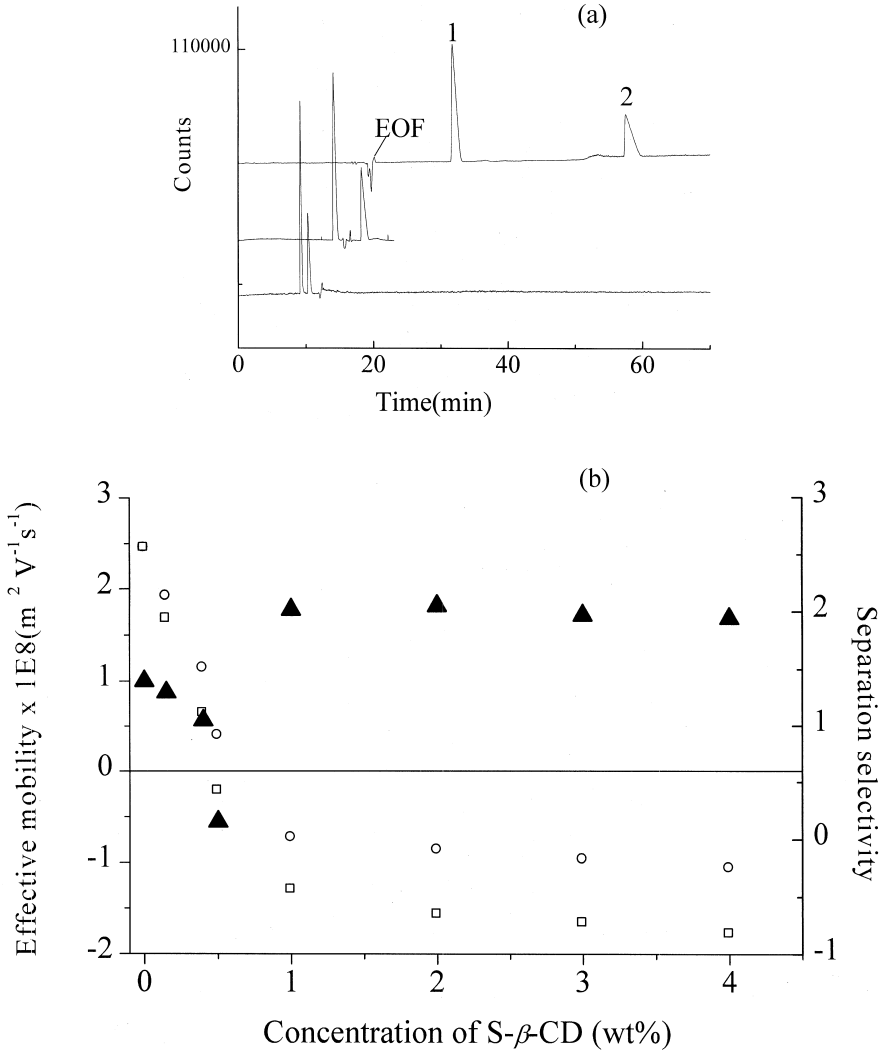

Fig. 3. (a) Electropherograms of the separation of *cis*-aminoindanol enantiomers using selected S-β-CD concentrations. Peak 1, (+)-*cis*-aminoindanol isomer; peak 2, (−)-*cis*-aminoindanol isomer. Conditions: 25 m*M* sodium phosphate BGE (pH 6.5) containing S-β-CD [0.3, 0.5 and 1.0% (w/w) for bottom, middle and top electropherograms], the applied voltage was kept at +15 kV, other conditions are the same as in Fig. 2. (b) Effect of the concentration of S-β-CD on enantiomer effective mobilities and separation selectivity, α, for the *cis*-aminoindanol enantiomers. Open circle, effective mobility of the (+)-*cis*-aminoindanol isomer; open square, effective mobility of the (−)-*cis*-aminoindanol isomer; solid up-triangle, α. Conditions are the same as in (a) except the concentration of the S-β-CD was varied from 0 to 4.0% (w/w).

the pH_{app} increased. This decrease can be attributed in part to the increase in ionic strength of the BGE from the Na^+ ions as the BGE was not Na^+ balanced [5,25]. In addition, as the pH_{app} approached the pK_a of the enantiomers (6.0), they began to deprotonate, reducing the ion-pairing effect between the analytes and chiral selector [20]. Consequently, the overall complexation between analytes and the S-β-CD becomes weaker, leading to a net decrease of the negative charge of the enantiomers–S-β-CD complexation, hence, the anionic electrophoretic mobility becomes slower. From these results it is

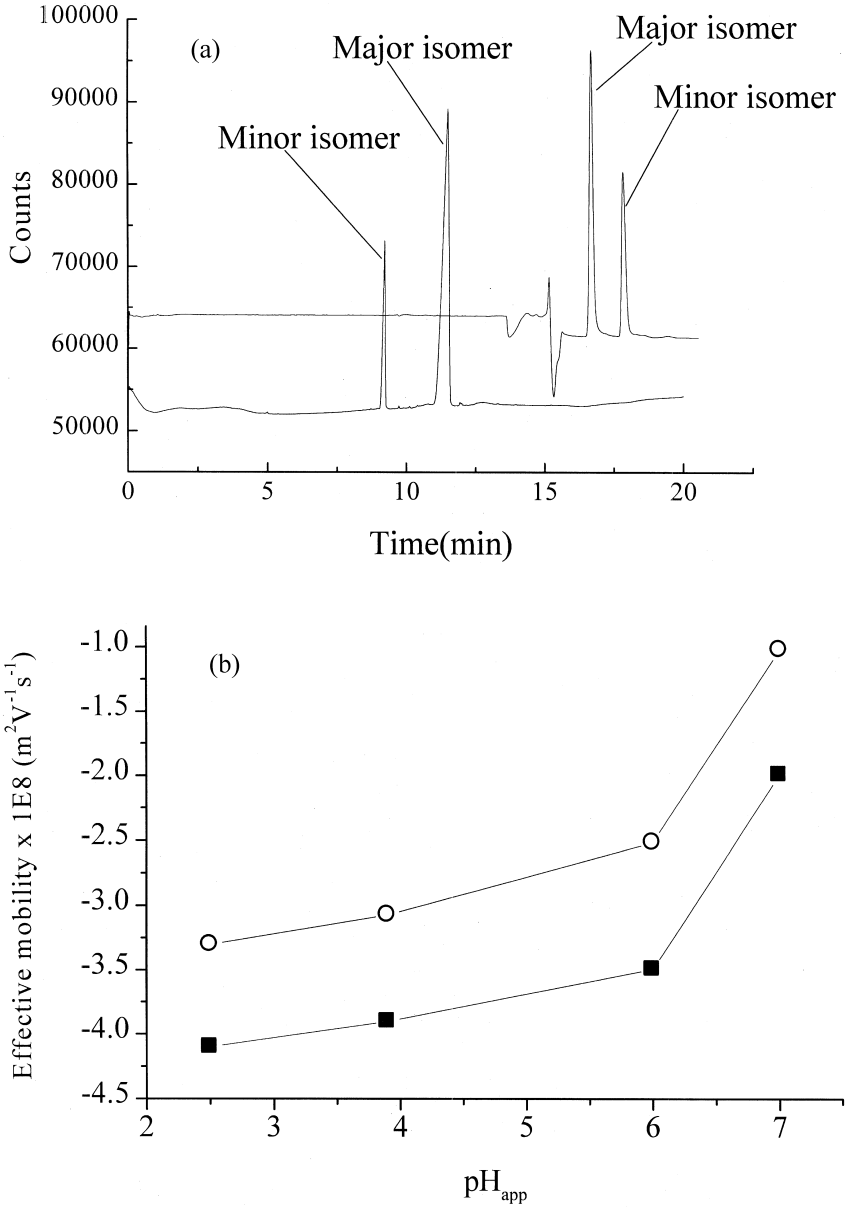

Fig. 4. (a) Effect of the pH_{app} on the separation and the elution order for compound I. Conditions: the BGE used for the upper electropherogram was 1.5% (w/w) S-β-CD in pH 9.3 Tris–borate buffer (25 m*M*) and the applied voltage was +15 kV, the BGE used for the bottom electropherogram was 1.5% (w/w) S-β-CD in pH 2.5 sodium phosphate buffer (25 m*M*) and the applied voltage was −15 kV. (b) Effect of the pH_{app} on the enantiomer effective mobilities for compound I and its minor enantiomer. Open circle, effective mobility of the minor isomer; solid square, effective mobility of the major isomer. Capillary: PVA coated 64.5 cm (effective length 56 cm)×50 μm I.D. at 30°C, the applied voltage was −15 kV and the concentration of the S-β-CD was 1.5% (w/w) and pH_{app} was varied, other conditions are the same as in Fig. 2.

also clear that both inclusion and electrostatic interactions are important for enantiomer–S-β-CD complexation.

3.4. Reversal of enantiomer elution order

In the chromatographic enantiomeric analysis of pharmaceutical compounds, it is typically desired to have the minor enantiomer elute in front of the major enantiomer, from practical standpoint. If the desired elution order is not achieved, the tail of the major enantiomer can cause interference towards the detection of minor amounts of the undesired enantiomer because of the large sample loading required to detect the minor enantiomer at the 0.1 area% level. Based on our study, we found the elution order of two enantiomers can easily be reversed by simply reversing the applied polarity or changing the pH of the BGE. As previously discussed, when compound I and its enantiomer are fully ionized (BGE pH 2.5), the effective mobility transitions from cationic to anionic. Therefore, the elution order of the enantiomers was opposite when the ''normal'' polarity was used for the cationic complexed enantiomers and ''reversed'' polarity was used for the anionic complexed enantiomers. The alternative way to reverse the elution order is to increase the pH of the BGE, forcing the analytes to elute solely by the EOF. As demonstrated in Fig. 4a, two electropherograms of the enantiomeric separation demonstrated opposite elution orders. The top one was achieved at elevated pH (pH 9.3), and the bottom one was achieved at lower pH (pH 2.5). Since the concentration of the S-β-CD is 1.5% (w/w) for both BGEs, both of the enantiomers effective mobilities were anionic. At elevated pH BGE, when ''normal'' polarity was applied, both of the resolved complexed enantiomers were forced to elute solely by the EOF. The stronger-binding complex peak carries more negative charge, hence eluting out later. In contrast, under low-pH buffer BGE, when ''reversed'' polarity was applied, the weaker-binding complex enantiomer had less negative charge and hence eluted out later. Therefore, the elution order of the enantiomeric separation was reversed. It is noticeable that the peak shape of the major isomer appears better in the higher pH buffer. The improvement in efficiency can be attributed to minimizing any analyte–capillary wall secondary interactions because the basic enantiomers are essentially neutral as the pH of the BGE was two units above the compounds' pK_a. However, the lower pH condition was selected for the final method because it provided the desired elution order.

3.5. Effect of the organic modifiers on the separation

Four common organic modifiers, MeOH, EtOH, IPA and ACN were added to the BGE within a 0–30% (v/v) range. The experiments were carried out using a PVA coated capillary. The change of the EOF was negligible for all organic modifiers. In all cases, the migration times of the analyte increased as the amount of the organic modifier in the BGE increased. This behavior can be attributed to either changes in the viscosity (η) or weakening of the affinity of the analytes for S-β-CD. It is recognized that organic modifiers compete with analyte for the relatively hydrophobic cavity of S-β-CD [5], therefore the complexation between the analyte and S-β-CD is reduced. Consequently, with reduction of the overall negative charge, at the reversal polarity mode, the migration time increased. As might be expected for a molecule with large hydrophobic regions, IPA should interact with the hydrophobic interior of the S-β-CD more strongly than EtOH and MeOH. Fig. 5 showed a clear trend as expected. The difference of ACN's effect on the separation may due to its aprotic solvent nature.

3.6. Effect of the temperature on the separation

The effect of increasing the separation temperature resulted in a decrease of the absolute effective mobilities. The plots of the effective mobilities vs. $1/T$ demonstrated a linear relationship with $r^2=0.99$ for both enantiomers (Fig. 6). The effect of the temperature is consistent with the literature. Kuhn and Erni estimated the thermodynamic values of the enantiomeric separation on CE using crown ether chiral selector based upon the linear plot of ln α vs. $1/T$ [26]. However, it is still controversial whether the direct application of the ''log α vs. $1/T$'' as a Van't Hoff plot is appropriate because the CE process is dependent upon the current, especially

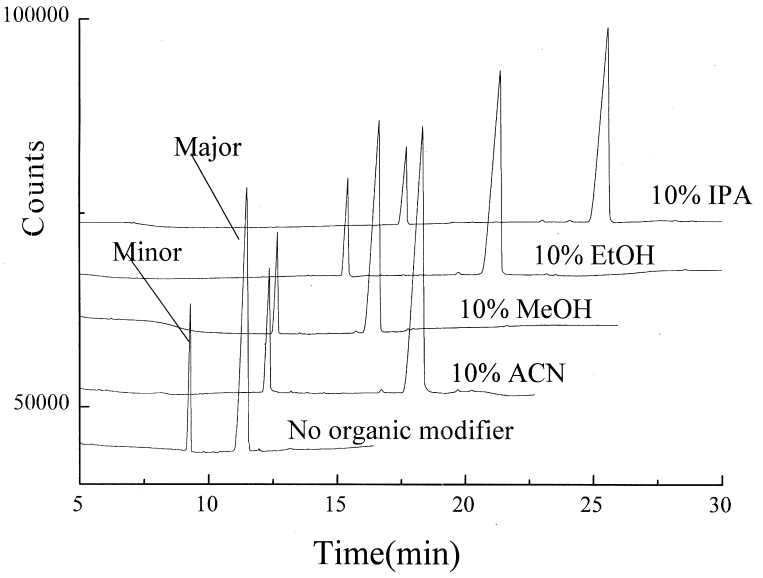

Fig. 5. Electropherograms of compound I and its enantiomer using selected organic modifiers. The BGE used for the electropherogram was 1.5% (w/w) S-β-CD in pH 2.5 sodium phosphate buffer (25 m*M*) except the organic modifiers were varied. The applied voltage was −15 kV.

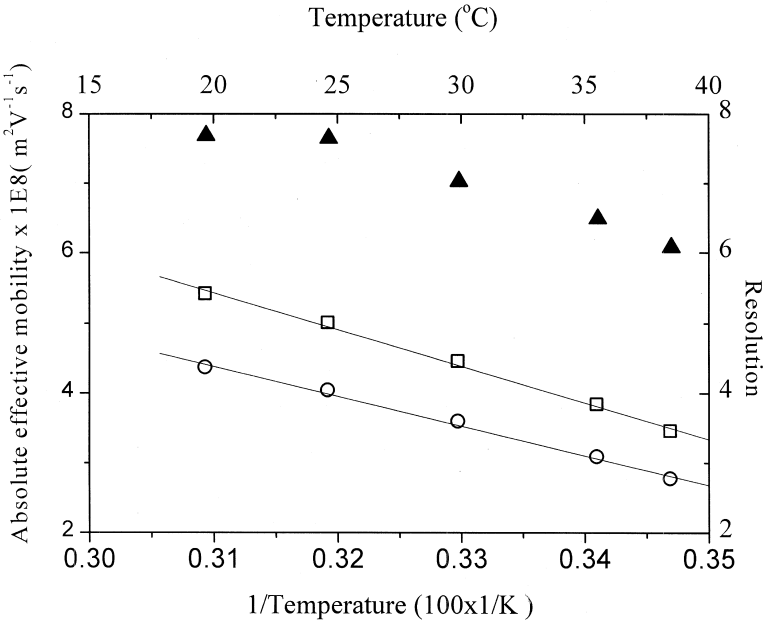

Fig. 6. Effect of temperature on the separation of compound I. Open circle, effective mobility of the minor isomer; open square, effective mobility of the major isomer; bottom *x*-axis, 1/*T*(100·1/K); solid up-triangle, resolution; upper *x*-axis, *t* (°C). Conditions are the same as the bottom electropherogram in Fig. 4a except the temperature was varied.

when charged chiral additives are used. It can be speculated that the linearity of Fig. 6 reflects the constancy over this temperature range of the interactions of the enantiomers with the S-β-CD [5]. Additionally, the resolution increased as the temperature decreased with a parallel sacrifice in the run time and the peak shape. Since there was sufficient resolution between the enantiomers at any of the temperatures evaluated, a temperature of 30°C was chosen for the final method.

3.7. Effect of buffer concentration and buffer type on the separation

Since the S-β-CD is fully ionized in the buffer solution, it contributes significantly to the ionic strength of the BGE. Therefore, the change in concentration of the sodium phosphate buffer from 15 m*M* to 50 m*M* has an insignificant impact on the effective mobility and resolution. However, changing the buffer counterion from sodium to TEA (at the same molar concentration and pH) has a significant influence on the separation. As shown in Fig. 7, the resolution dramatically increased while the mobility of the enantiomers decreased when utilizing the TEA–phosphate BGE. Vincent and Vigh measured the EOF for the TEA–phosphate BGE with and without HDAS-β-CD [18]. Their results revealed that there was significant TEA adsorption on the capillary wall with the absence of the HDAS-β-CD. The EOF was anionic initially, but as the concentration of HDAS-β-CD increased, the EOF became cationic. Since the concentration of S-β-CD was elevated in both sodium phosphate and TEA–phosphate BGEs in our study, the TEA effect due to absorbance on the wall should be negligible. In addition, under ''reversed'' polarity, the mobilities of the anionic complexes would increase if there was an anionic EOF present. Therefore, the separation behavior that we observed may be attributed in part due to the change in electromigration dispersion as the effective mobility of anionic S-β-CD enantiomer complex is decreased through ion pairing with TEA [22,27]. Such interactions would result in reducing the net negative charge and increasing the hydrodynamic size of the S-β-CD–enantiomer complexes.

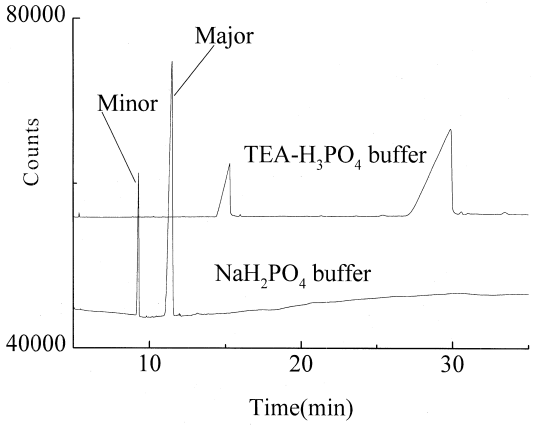

Fig. 7. Electropherograms of compound I and its enantiomer using different buffers. Conditions: the BGE used for the upper electropherogram was 1.5% (w/w) S-β-CD in TEA–phosphate buffer (25 m*M*, pH 2.5), the other conditions are the same as the bottom electropherogram in Fig. 4a.

3.8. Effect of voltage on the separation

The effective mobilities of the analytes should be independent of the applied voltages. We observed that the effective mobilities were almost constant in the range from 5 to 20 kV (Fig. 8). However, they started to increase when the voltage was set higher than 20 kV. This behavior is due to the excessive Joule heating [23] generated during the electrophoresis process because the negatively charged S-β-CD has a large contribution to the current. This result is also confirmed by the nonlinear behavior of the Ohm's law plot as shown in Fig. 8.

3.9. Method validation

After systematic method optimization, the final method conditions were as follows: a BGE of 25 m*M* low-pH sodium phosphate buffer (pH 2.5) with 1.5% (w/w) S-β-CD, an applied voltage of −15 kV (''reversed'' polarity) and a fused-silica capillary temperature control of 30±0.1°C (typical current approximately 65 μA). In order to demonstrate that the method was practical, a validation study was performed.

3.9.1. Lot-to-lot reliability of the S-β-CD

The lot-to-lot reliability of the S-β-CD was evaluated, because of the observed differences in the

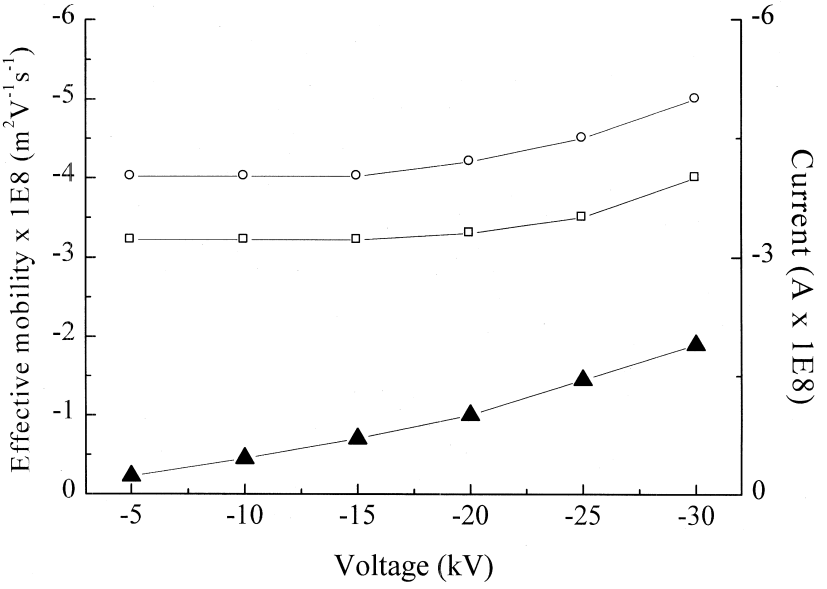

Fig. 8. Effect of the applied voltage on the effective mobilities for compound I and its minor enantiomer. Open circle, effective mobility of the minor isomer; open square, effective mobility of the major isomer; up-triangle, Ohm's law plot. Conditions are the same as the bottom electropherogram in Fig. 4a except the applied voltage was varied.

minor impurities found in different lots of the S-β-CD by CE–indirect UV detection evaluations and the random sulfation. Three lots of S-β-CD obtained from Aldrich were used for the study. As can be seen from Table 1, the reproducibility of the migration time of both enantiomers obtained by using three different lots of the S-β-CD is excellent. The relative standard deviations (RSDs) of migration times of both enantiomers for eight injections (duplicate injections for each sample) are less than 1.5%. These results indicated that the method variation caused by batch-to-batch S-β-CD (from Aldrich) variation is negligible for this application.

Table 1
Evaluation of the lot to lot variability of the chiral selector

Lot #	Sample #	MT-UT	MT-D
JR09718HR	JR1-1	9.301	11.502
	JR1-2	9.292	11.488
	JR2-1	9.289	11.482
	JR2-2	9.246	11.394
LS09918HR	LS1-1	0.247	11.392
	LS1-2	9.235	11.394
HU05208HO	HU1-1	9.255	11.447
	HU1-2	9.012	10.989
Average		9.235	11.386
%RSD		1.0	1.3

Conditions are the same as provided for the bottom electropherogram in Fig. 4a. Key: MT-UD: migration of undesired enantiomer; MT-D: migration of desired enantiomer; Sample #: JR(lot)1(preparation #)−1(injection #).

3.9.2. Robustness

The method was performed by different chemists on different instruments with different capillary lots on different days. The changes of the migration times of both enantiomers were within a ±1 min window with all these variations. This performance is superior to most LC chiral column separation methods. The migration times of both enantiomers gradually increased and the separation efficiency decreased as the same vial of the running buffer was repeatedly used. Therefore, we recommend replenishing the running buffer after every two runs.

3.9.3. Limits of detection (LODs) and quantitation (LOQs)

One of the most important aspects for isomeric impurity determination method validation is detection sensitivity. The detection sensitivity can be demonstrated by the LOD. The LOD was determined

through a linearity study (R^2>0.99) of a series dilution of compound I over the range from 0.1% to 125% of the target concentration (0.5 mg/ml). At the concentration of 0.1%, the injected solution produced a signal-to-noise ratio of 3. In addition, an aliquot of minor enantiomer was spiked into the sample of pure compound I at 0.1% of the target concentration level. As we can see from Fig. 9, the minor peak has a signal-to-noise ratio of 5 at the 0.1% level and is clearly detectable.

The LOQ was found to be 0.3% of target concentration (0.5 mg/ml) based on the satisfaction of three criteria: (A) the S/N ratio of the LOQ (0.3%) solution was greater than 10; (B) the percent difference of response factor values at the LOQ and 5×LOQ was less than 20; (C) the RSD of area counts for three injections at the LOQ level was less than 15%.

3.9.4. Precision and accuracy

A 0.5 mg/ml sample of compound I was spiked with the minor enantiomer at 0.1, 0.5 and 1.0% (w/w) levels. The 0.5% (w/w) level spiked solution was injected six times consecutively. As shown in Table 2, the RSD of quantitation was 0.01% for compound I and 3.3% for the minor enantiomer based on the area%.

Accuracy was determined by calculating the recovery of the minor enantiomer at 0.1, 0.5 and 1.0% of the target concentration levels. The average recovery of the minor enantiomer is 102% as shown in Table 3. Additionally, an independent HPLC analysis of the same sample solution using a chiral α_1-acid glycoprotein column confirmed the accuracy of the CE results.

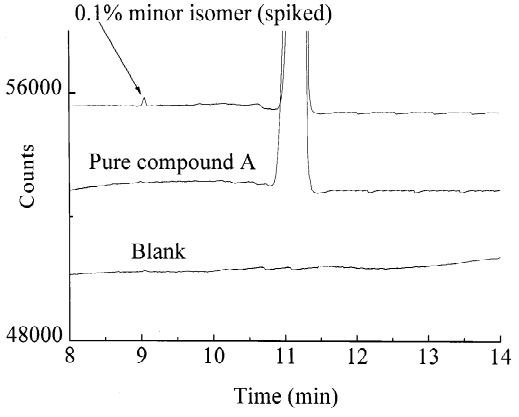

Fig. 9. Electropherogram of pure compound I and pure compound I spiked with 0.1% of the minor enantiomer. Conditions are the same as the bottom electropherogram in Fig. 4a.

Table 2
The injection precision of the method

Replicate injections number	Area % of major isomer	Area % of minor isomer
1	99.565	0.435
2	99.539	0.461
3	99.524	0.476
4	99.551	0.449
5	99.555	0.445
6	99.556	0.444
Average	99.548	0.452
% RSD	0.015	3.264

Conditions are the same as for Table 1.

4. Conclusions

A simple, fast, accurate, precise, rugged and sensitive chiral CE method with desired selectivity was achieved using randomly S-β-CD through a systematic approach to method development based on theoretical predictions. Therefore, the enantiomeric purity of compound I can be quantitatively determined. Future work will explore developing a general strategy for method development that can be applied towards the enantiomeric separation of other pharmaceutically related compounds by CE.

Table 3
Recovery study for the minor enantiomer

$C_{spiking}$ (%)	Recovery (%)
0.1	108.7
0.5	97.8
1.0	100.3
Average	102.3

$C_{spiking}$: concentration of the spiking solution. Conditions are the same as for Table 1.

Acknowledgements

The authors wish to thank the Merck Summer Internship Program that provided the support for C.M.

References

[1] S.C. Beale, Anal. Chem. 70 (1998) 279R.
[2] S. Fanali, J. Chromatogr. A 792 (1997) 227.
[3] R.L. St. Clarire, Anal Chem. 68 (1996) 569R.
[4] H. Nishi, J. Chromatogr. A 792 (1997) 327.
[5] L. Zhou, J. Trubig, A. Dovletoglou, D. Locke, J. Chromatogr. A 773 (1997) 311.
[6] L. Zhou, R. Thomposon, D. Ellison, D. Locke, J. Cap. Electrophoresis 6 (1997) 279.
[7] S. Terabe, Trends Anal. Chem. 8 (1989) 129.
[8] A. Nardi, A. Eliseev, P. Bocek, S. Fanali, J. Chromatogr. 638 (1993) 247.
[9] S.A.C. Wren, R. Rowe, J. Chromatogr. A 603 (1992) 235.
[10] S.G. Penn, E.T. Bergström, D.M. Goodall, J.S. Loran, Anal. Chem. 66 (1994) 2866.
[11] Y. Rawjee, D.U. Staerk, G. Vigh, J. Chromatogr. A 635 (1993) 291.
[12] Y. Rawjee, D.U. Staerk, G. Vigh, J. Chromatogr. A 652 (1993) 233.
[13] Y. Rawjee, D.U. Staerk, G. Vigh, J. Chromatogr. A 688 (1994) 273.
[14] B. Williams, G. Vigh, J. Chromatogr. A 777 (1997) 295.
[15] J.B. Vincent, A.D. Sokolowski, T.V. Nguyen, G. Vigh, Anal. Chem. 69 (1997) 4226.
[16] J.B. Vincent, A.D. Sokolowski, T.V. Nguyen, G. Vigh, Anal. Chem. 69 (1997) 4419.
[17] J.B. Vincent, A.D. Sokolowski, T.V. Nguyen, G. Vigh, Anal. Chem. 70 (1998) 580.
[18] J.B. Vincent, G. Vigh, J. Chromatogr. A 817 (1998) 105.
[19] K.H. Gahm, A.M. Stalcup, Chirality 8 (1996) 316.
[20] K.H. Gahm, A.M. Stalcup, Anal. Chem. 68 (1996) 1360.
[21] F. Wang, M.G. Khaledi, J. Microcol. Sep. 11 (1999) 11.
[22] B. Williams, G. Vigh, Anal. Chem. 68 (1996) 1174.
[23] J.W. Jorgenson, K.D. Lukacs, Anal. Chem. 53 (1981) 1298.
[24] C. Desiderio, S. Fanali, J. Chromatogr. A 716 (1998) 183.
[25] Y.Y. Rawjee, R.L. Williams, G. Vigh, Anal.Chem. 66 (1994) 3777.
[26] R. Kuhn, F. Erni, Anal. Chem. 64 (1992) 2815.
[27] R. Williams, B. Childs, E.V. Dose, G. Guiochon, G. Vigh, J. Chromatogr. A 781 (1997) 107.